

# Metastable-atom-activated growth of an ultrathin carbonaceous resist for reactive ion etching of SiO<sub>2</sub> and Si<sub>3</sub>N<sub>4</sub>

J. H. Thywissen,<sup>a)</sup> K. S. Johnson, N. H. Dekker, and M. Prentiss  
*Department of Physics, Harvard University, Cambridge, Massachusetts 02138*

S. S. Wong  
*Department of Chemistry and Chemical Biology, Harvard University, Cambridge, Massachusetts 02138*

K. Weiss and M. Grunze  
*Angewandte Physikalische Chemie, Universität Heidelberg, Im Neuenheimer Feld 253,  
D 69120 Heidelberg, Germany*

(Received 22 October 1997; accepted 6 February 1998)

A thin carbonaceous resist was grown by exposing a substrate to a beam of neutral metastable argon atoms in the presence of siloxane vapor. X-ray photoelectron spectroscopy and Auger electron spectroscopy data show that the resist was composed primarily of carbon. Near edge x-ray absorption fine structure spectra of samples exposed to metastable atoms show that carbon double bonds were formed during exposure. The deposited material was used as a resist for reactive ion etching into SiO<sub>2</sub> and Si<sub>3</sub>N<sub>4</sub>. Lines in SiO<sub>2</sub> were fabricated with widths as small as 20 nm, aspect ratios >2:1, and sidewalls as steep as 7:1. © 1998 American Vacuum Society.  
[S0734-211X(98)04103-1]

## I. INTRODUCTION

Neutral atom lithography can create permanent structures with small feature sizes and excellent registration by patterning a thermal beam of atoms incident on a surface.<sup>1,2</sup> Tools for the manipulation and patterning of neutral atomic beams are provided by the growing field of atom optics: available tools include beam brighteners, lenses, mirrors, and masks.<sup>3</sup> Recent progress in atom lithography has included the demonstration of resists sensitive to neutral atoms, and the transfer of patterns into a variety of substrates;<sup>4-7</sup> these same resists also serve as high spatial-resolution, high sensitivity detectors for atoms. In this work, a carbonaceous resist material is formed by exposing a substrate to neutral metastable argon (Ar\*) atoms in the presence of a siloxane vapor. The composition and structure of the carbonaceous material are analyzed, and the resist is used as an etch mask for dry pattern transfer into SiO<sub>2</sub> and Si<sub>3</sub>N<sub>4</sub> substrates.

Neutral metastable atoms have several attractive features as a patterning agent in a lithographic system. (1) Neutral atomic beams with thermal kinetic energies (~50 meV) have short de Broglie wavelengths (<1 Å). (2) A noble gas atom in a metastable excited state<sup>8</sup> is de-excited upon interaction with a substrate and releases its 12 eV (in the case of Ar\*) of internal energy into the top few nm of the substrate.<sup>9,10</sup> (3) The dissipation of the internal energy of a metastable atom can be initiated by a single IR photon before the atom reaches a surface. This process converts a metastable atom, which contains sufficient energy to damage a resist or affect a surface, into a ground state atom, which is chemically inert.<sup>4,11</sup> (4) Laser light fields can serve both as lens arrays<sup>1</sup> and as periodic amplitude gratings<sup>12,13</sup> that pattern atomic beams; both atom optical elements exhibit excel-

lent long-range registration, with a period referenced to atomic frequency standards. (5) Neutral atoms can pattern ultrathin (<5 nm thick) layers which have demonstrated sub-10 nm resolution.<sup>14,15</sup>

Previous work has demonstrated lithographic techniques that use metastable atoms to activate selectively the deposition of a carbonaceous resist in a pattern that is subsequently transferred into an underlying substrate.<sup>11,16</sup> Upon impact, metastable atoms transfer energy into physisorbed hydrocarbons and induce a chemical change that results in the formation of a durable material. Circular features with a diameter of 50 nm were created using a stencil mask to pattern a beam of neutral metastable atoms. Patterns were transferred from the deposited material into Si, SiO<sub>2</sub>, and Au by wet chemical etching<sup>11</sup> and into GaAs by chemically assisted ion beam etching.<sup>16</sup>

In this work, we find that the carbonaceous material formed by exposing a substrate to metastable atoms was similar in composition to the "contamination" material formed by exposing a substrate to electron beams.<sup>15</sup> Furthermore, we show that the chemical bonds in the metastable-formed material are similar to those created by low-energy electron irradiation of a polymer: recent near edge x-ray absorption fine structure (NEXAFS) measurements on self-assembled monolayers (SAMs) showed conclusively that low-energy electron irradiation leads to dissociation of carbon-hydrogen bonds and formation of intramolecular, unsaturated, C=C double bonds.<sup>17-19</sup> The NEXAFS spectra we present here suggest that a similar process has occurred in samples exposed to metastable atoms.

The spatial resolution, metastable-activated growth rate, and etch properties of the deposited material are also investigated. We report the transfer of patterns from the grown material into SiO<sub>2</sub> and Si<sub>3</sub>N<sub>4</sub> via reactive ion etching (RIE) with CH<sub>3</sub>. The features etched into SiO<sub>2</sub> show that the depo-

<sup>a)</sup>Electronic mail: joseph@atomsun.harvard.edu

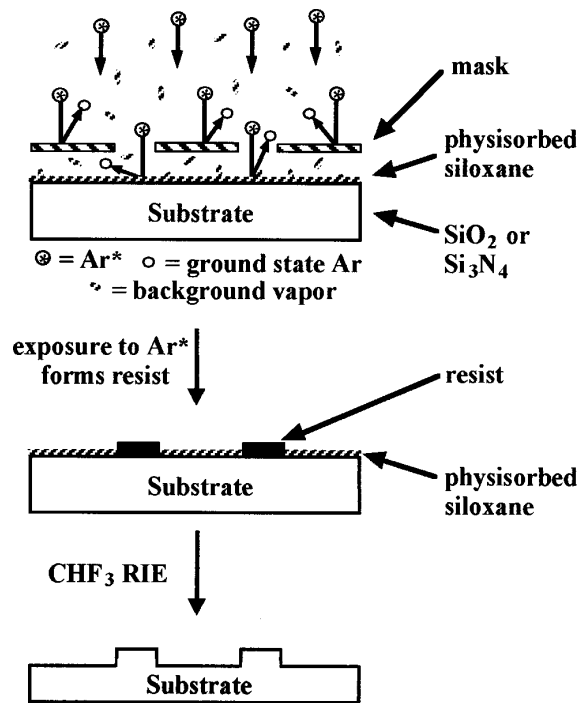


FIG. 1. Schematic diagram of the lithographic process (not to scale). Substrates were exposed to a beam of neutral metastable argon atoms that had been patterned by a stencil mask. The environment was a vacuum ( $3 \times 10^{-7}$  Torr) containing a vapor of siloxane oil. Carbonaceous material was formed in the regions exposed to the metastable atoms. The pattern was transferred into the underlying SiO<sub>2</sub> or Si<sub>3</sub>N<sub>4</sub> substrates by CHF<sub>3</sub> RIE.

sition and etching process can create 20 nm features, >2:1 aspect ratios, steep sidewalls, and smooth etched surfaces. Our results indicate that the deposited carbonaceous material serves as a robust etch mask against high energy ( $\sim 1$  keV) ions. This durability is attributed to the observed presence of carbon double bonds in the material after exposure to metastable atoms.

## II. EXPERIMENT

Figure 1 shows the process used to pattern SiO<sub>2</sub> and Si<sub>3</sub>N<sub>4</sub> layers. Substrates were exposed to a beam of Ar\* atoms in the presence of background vapors of siloxane diffusion-pump oil.<sup>20</sup> The flux of Ar\* hitting the substrate was  $3 \times 10^{12}$  atoms cm<sup>-2</sup> s<sup>-1</sup>; this flux measurement assumes an efficiency of 0.2 ejected electrons per Ar\* atom incident on a graphite-coated surface.<sup>21</sup> The beam apparatus has been described previously.<sup>11</sup>

Samples were exposed to the atomic beam through one of two different stencil masks. The first mask, used to create arrays of lines with a period of 100 nm, was a Si<sub>3</sub>N<sub>4</sub> membrane fabricated by Savas *et al.* using UV achromatic interferometric lithography<sup>22</sup> (AIL). The second stencil mask was a simple stainless steel mesh, used to create macroscopic patterns for measurement of growth rates, etch rates, and etch selectivities.

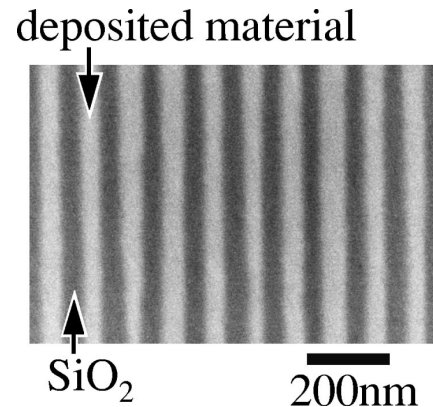


FIG. 2. Scanning electron micrograph of deposited material before transfer into the underlying SiO<sub>2</sub> substrate. The material was deposited in regions exposed to  $\sim 6 \times 10^{17}$  Ar\* atoms cm<sup>-2</sup>. The stencil mask that patterned the beam of metastable atoms was a free-standing grating with 100 nm period. Atomic force microscopy determined that the features are  $\sim 15$  nm tall.

X-ray photoelectron spectroscopy (XPS)<sup>23</sup> and Auger electron spectroscopy (AES)<sup>24</sup> were used to determine the elemental composition of the deposited material. NEXAFS spectroscopy was used to determine the chemical structure of the material.<sup>25</sup>

Following the metastable-activated deposition of material, samples were etched in a parallel-plate rf-driven reactive ion etching system. The electrode area was 200 cm<sup>2</sup>, and the powered electrode was covered by a quartz plate. The base pressure of the system was  $10^{-4}$  Torr. Between etches, the electrodes were scrubbed, wiped with isopropanol, and cleaned with an oxygen plasma run for  $\sim 10$  min at 100 W, 50 sccm, and 170 mTorr. The samples were then placed in the chamber and etched with CHF<sub>3</sub>, at powers between 50 and 150 W, flows between 15 and 25 sccm, average substrate self-biases between 600 and 1100 V, and a pressure of  $\sim 30$  mTorr. A Tencor Alpha Step profilometer was used to measure step heights before and after etching.

Samples were imaged by a Gemini Leo field emission scanning electron microscope (SEM), a Park Scientific atomic force microscope (AFM) in contact mode using a tip  $\sim 40$  nm in diameter, and a Digital Instruments Nanoscope III Multimode AFM, operated in tapping mode with a carbon nanotube tip  $\sim 15$  nm in diameter.<sup>26</sup>

## III. RESULTS

### A. Analysis

Figure 2 shows a SEM image of 40–60-nm-wide carbonaceous lines formed by 54 h ( $\sim 6 \times 10^{17}$  atoms cm<sup>-2</sup>) of exposure to Ar\* through the AIL stencil mask. In effect, an atomic beam was used to create a high-resolution copy of the stencil mask in a process analogous to the use of light to

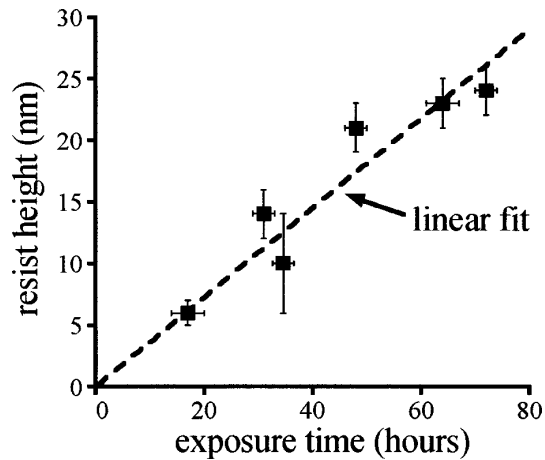


FIG. 3. Deposited layer thickness, measured by profilometry, vs exposure time to  $\text{Ar}^*$ . One hour of exposure time corresponds to  $\sim 10^{16}$  atoms  $\text{cm}^{-2}$  and the delivery of  $\sim 20$  mJ  $\text{cm}^{-2}$  to the surface. Each point corresponds to one exposure. A least squares linear fit gives an average deposition rate of  $0.34 \pm 0.04$  nm/h.

record an image onto photographic film. Subsequent etching (described below) provides contrast enhancement of this neutral atom photograph.

Figure 3 shows the thickness of grown material versus length of exposure to metastable atoms. The average deposition rate, as determined by a least squares linear fit, was  $0.34 \pm 0.04$  nm/h and was constant over a wide range of exposure times. The growth rates on Au,  $\text{SiO}_2$ , and  $\text{Si}_3\text{N}_4$  were found to be the same. Comparing this metastable-activated growth rate to typical 50 kV electron-assisted contamination growth rates<sup>14,27</sup> of  $\sim 1$  nm per 10 C  $\text{cm}^{-2}$  exposure, we estimate the growth rate per incident particle to be  $\sim 2000$  times higher for  $\text{Ar}^*$  than for 50 kV electrons, and the growth rate per unit energy incident upon the surface to be  $> 10^6$  times higher for  $\text{Ar}^*$  than for 50 kV electrons.

Figure 4 presents compositional and structural information about the material grown on the surface. Figure 4(a) shows XPS spectra for exposed and unexposed regions of the same  $\text{SiO}_2$  substrate. After a 21 h exposure, the carbon 1s photopeak increased in intensity by a factor of  $2.6 \pm 0.3$ , whereas the oxygen 1s and silicon 2p peaks decreased by factors of  $4.7 \pm 0.4$  and  $3.5 \pm 0.6$ , respectively. We attribute this behavior to the deposition of a C/Si/O material that is thicker than the escape depth of the photoelectrons,  $\sim 30$  Å. Because the Si and O are present in much lower concentrations in the resist than in the  $\text{SiO}_2$  substrate, their XPS peaks are correspondingly lowered. AES spectra of an exposed gold substrate are consistent with this interpretation: in regions where the underlying gold substrate is fully occluded by the deposited material, the surface composition was 88% carbon, 4% silicon, and 8% oxygen. Since carbon, silicon, and oxygen are the primary constituents of the siloxane vapor, these results suggest that the diffusion-pump oil vapor is the source of the deposited material.<sup>28</sup>

Figure 4(b) shows the NEXAFS spectra of five samples,

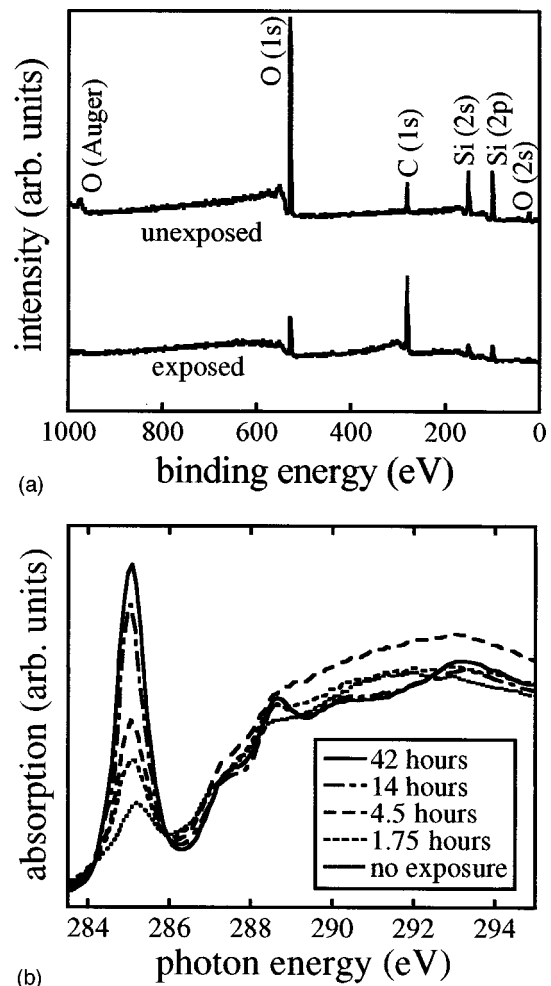


FIG. 4. (a) XPS spectra of two regions on a  $\text{SiO}_2$  substrate: the C (1s) peak is  $2.6 \pm 0.3$  times more intense in the region that has been exposed to  $2 \times 10^{16}$   $\text{Ar}^*$  atoms  $\text{cm}^{-2}$  (lower curve) than in the region that was masked from exposure (upper curve); the Si(2s) and O(1s) peaks have decreased by similar factors. (b) NEXAFS spectra of resist layers formed on a gold surface by 0, 1.75, 4.5, 12, and 42 h of exposure time at a flux of  $\sim 10^{16}$   $\text{Ar}^*$  atoms  $\text{cm}^{-2}$   $\text{h}^{-1}$ . The growth of a sharp peak at 285.1 eV with increasing exposure time indicates the formation of material with C=C bonds.

each of which had a different  $\text{Ar}^*$  exposure time. The spectra were recorded at  $54^\circ$ , the “magic angle” at which effects due to the polarization of the incident synchrotron radiation cancel out.<sup>29</sup> NEXAFS probes the density of unoccupied states, and reveals the presence of  $\pi$  orbitals associated with unsaturated carbon–carbon bonds with high sensitivity. In particular, the resonance at 285.1 eV photon energy increases with increased exposure to the beam of  $\text{Ar}^*$ , and is identified as a C 1s  $\rightarrow \pi^*$  transition characteristic of C=C double bonds.<sup>29</sup> C=C double bond formation has previously been observed by NEXAFS analysis of SAMs exposed to electrons of kinetic energy similar to the internal energy of the metastable atoms, 10–100 eV.<sup>17–19</sup> In conjunction, these two observations suggest that the growth mechanism of the resist involves the dissociation of C–H bonds and the formation of alkene moieties in the hydrocarbon material.

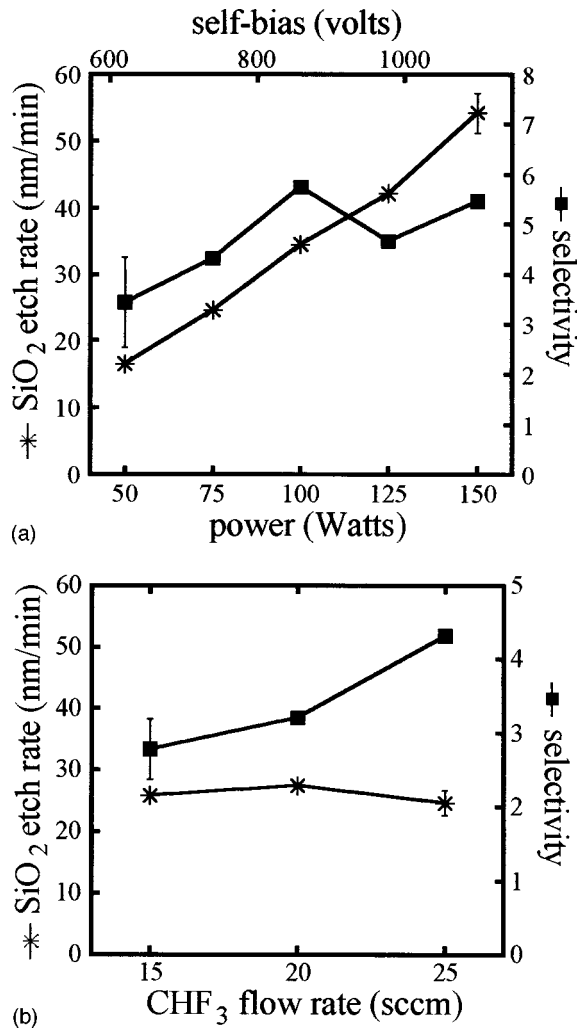


FIG. 5. Average etch rates of SiO<sub>2</sub> and average etch rate ratio ("selectivity") of SiO<sub>2</sub> to deposited material. A representative error bar is shown for each curve. (a) Etch rate and selectivity vs rf power at 25 sccm flow rate of CHF<sub>3</sub>, 30 mTorr pressure. The self-bias of the substrate was observed to be a roughly linear function of power, as plotted on the upper axis. (b) Average etch rate and selectivity vs flow rate of CHF<sub>3</sub> at 75 W, 780 ± 20 V self-bias. We were experimentally limited to a flow rate no greater than 25 sccm.

## B. Etching

In order to optimize the reactive ion etching parameters, we studied the etch rate of SiO<sub>2</sub> and the etch selectivity of SiO<sub>2</sub> with respect to the carbonaceous resist as a function of rf power and CHF<sub>3</sub> flow rate. Figure 5(a) shows that the etch selectivity of SiO<sub>2</sub> with respect to C increased with increasing power up to 100 W. Note that 5:1 etch selectivity was observed for a self-bias as large as 1.1 kV, corresponding to a substantial energy of ion bombardment during the etch. In contrast, the dry etching of other thin carbonaceous layers, such as SAMs,<sup>30</sup> requires a very low bias for selective etching conditions. We attribute the durability of the metastable-formed material to graphitic structure, as suggested by the presence of a carbon double bond resonance in the NEXAFS data. Materials with higher C:H ratios are known to exhibit higher dry etch resistances than saturated hydrocarbon materials.<sup>31</sup>

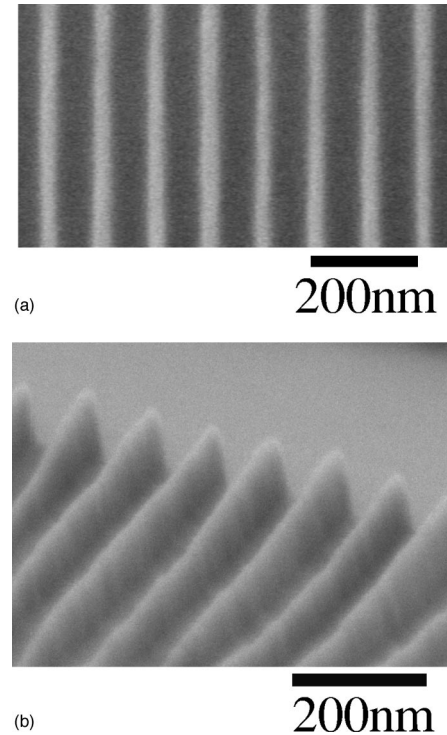


FIG. 6. Features (white in this image) transferred into SiO<sub>2</sub> by RIE. Views are (a) normal incidence and (b) at a 75° angle. Both samples were exposed to Ar\* for 54 h and then etched with the parameters (a) 150 W power, 1100 V self-bias, 25 sccm flow of CHF<sub>3</sub>, 30 mTorr pressure, 2 min and (b) 100 W power, 860 V bias, 25 sccm flow of CHF<sub>3</sub>, 30 mTorr pressure, 2 min. The features shown in (b) have an aspect ratio of greater than 2:1.

Figure 5(b) shows increased selectivity at higher CHF<sub>3</sub> flow rates. The increased selectivity is due to a reduced etch rate of the resist, which can be explained by the role of fluorocarbon polymers in the plasma. Potter *et al.*<sup>32</sup> have shown that the reactive ion etch rate of Si in a CHF<sub>3</sub> plasma is limited by the rate of fluorine diffusion through a steady-state fluorocarbon layer on the Si surface. SiO<sub>2</sub> is selectively etched faster than non-oxygen-containing surfaces such as Si, or C in our system, because the oxygen in SiO<sub>2</sub> prevents the formation of a similar inhibiting polymer on its surface. At higher pressures and flow rates, the steady-state layer of fluorocarbon polymer formed on Si was shown to be thicker, further slowing the diffusion of fluorine to the Si surface. The resist layer in our system behaves similarly to Si in Potter's analysis because the material contains only a small fraction of O.

Figure 6 shows SEM images of lines etched into SiO<sub>2</sub> samples after a 54 h exposure ( $\sim 6 \times 10^{17}$  atoms cm<sup>-2</sup>) to a beam of metastable atoms patterned by the AIL stencil mask. Figure 6(a) shows lines with widths as small as 20 nm, after etching for 2 min with CHF<sub>3</sub> at 150 W and 25 sccm. These lines were measured by AFM to be 40 nm tall. Figure 6(b) shows a profile view of features in SiO<sub>2</sub> fabricated by etching for 3 min with CHF<sub>3</sub> at 100 W and 25 sccm. These features were  $\sim 80$  nm tall and  $\sim 35$  nm wide. The difference in linewidth between the samples shown in Figs. 6(a) and 6(b) may be due to differing etch conditions or due to varia-

tions in the pattern transmitted by the stencil mask.

The profiles of the etched lines shown in Fig. 6(b) were also measured by AFM. For a surface formed by etching  $\sim 80$  nm down into the  $\text{SiO}_2$ , we measured a rms roughness of the pedestal base of less than 3 nm. An AFM with a nanotube tip revealed profiles with flat tops and sidewalls as steep as 7:1, i.e., at roughly an  $82^\circ$  angle from horizontal.

We have also transferred macroscopic patterns from the resist into a  $\text{Si}_3\text{N}_4$  surface. At 125 W and 25 sccm, the etch rate ratio of  $\text{Si}_3\text{N}_4$ :resist was 7:1, and the average etch rate of  $\text{Si}_3\text{N}_4$  over a 3 min etch was  $45 \pm 5$  nm/min.

#### IV. CONCLUSIONS

In the presence of a background hydrocarbon vapor, exposure of substrates to neutral metastable atoms activates the growth of a carbonaceous material. We have shown that the height of this material grows linearly with exposure time, at a rate independent of the underlying substrate material. The resist material consisted of carbon, silicon, and oxygen as did its vapor precursor. The durability of this material during etching with  $\sim 1$  keV ions is attributed to its double-bonded structure.

Long exposure times ( $\sim 50$  h) were used to make the  $\sim 100$ -nm-tall structures shown in this work. Future efforts to reduce the required exposure time will include (1) increasing the flux of metastable atoms hitting the substrate, (2) using a more efficient combination of vapor precursor and metastable atom,<sup>16</sup> and (3) improving the selectivity of the etching process. The latter two approaches would also make the lithographic system a more sensitive detector of metastable atoms.

Dry etching is an improvement over the wet etches used in previous atom lithography systems because the etch can be made anisotropic, and because resist de-adhesion is less of a problem for dry etches.<sup>16</sup> In this work, we have obtained sidewalls as steep as 7:1, aspect ratios greater than 2:1, and linewidths as small as 20 nm. Furthermore, the characterization of the structure and RIE properties of the deposited material lays the groundwork for etches with higher selectivities and aspect ratios. For instance, high aspect ratio ( $> 25$ ) features have been created using  $\text{SiO}_2$  as an etch mask for Si.<sup>33</sup> Dry etching with chlorine of electron-beam-deposited contamination material on GaAs has demonstrated selectivities of  $> 30:1$ .<sup>27</sup> Similar chemistries may allow high aspect ratios and high selectivities in RIE systems using the resist described in this work.

#### ACKNOWLEDGMENTS

This work was supported in part by the NSF (PHY 9312572), and used MRSEC Shared Facilities supported by NSF under Award No. DMR-9400396. The NEXAFS study was supported by the German BMBF (05625 VHA). Fabrication of carbon nanotube tips and AFM using these tips were performed in the laboratory of Professor C. M. Lieber (Harvard University). J. T. was supported by the Fannie and John Hertz Foundation; K. J. by an AT&T/Lucent Graduate Fellowship; and S. W. by a NSREC (Canada) Postgraduate

Fellowship. The authors thank T. Savas and Henry I. Smith for providing the 100 nm period stencil masks used in this work; K. K. Berggren for guidance and careful editing; S. Shepherd, Yuanchang Lu, and L. Shaw for assistance in sample analysis; and R. Younkin, G. M. Whitesides, and C. Wöll for fruitful discussions.

<sup>1</sup>G. Timp, R. E. Behringer, D. M. Tennant, J. E. Cunningham, M. Prentiss, and K. K. Berggren, *Phys. Rev. Lett.* **69**, 1636 (1992); J. J. McClelland, R. E. Scholten, E. C. Palm, and R. J. Celotta, *Science* **262**, 877 (1993); R. W. McGowan, D. M. Giltner, and S. A. Lee, *Opt. Lett.* **20**, 2535 (1995); U. Drodofsky, J. Stuhler, B. Brezger, Th. Schulze, M. Drewsen, T. Pfau, and J. Mlynek, *Microelectron. Eng.* **35**, 285 (1997); F. Lison, H.-J. Adams, D. Haubrich, M. Kreis, S. Nowak, and D. Meschede, *Appl. Phys. B* **65**, 419 (1997).

<sup>2</sup>For a review of atom lithography, see J. H. Thywissen, K. S. Johnson, R. Younkin, N. H. Dekker, K. K. Berggren, A. P. Chu, M. Prentiss, and S. A. Lee, *J. Vac. Sci. Technol. B* **15**, 2093 (1997).

<sup>3</sup>For a review of atom optics and optical forces, see C. S. Adams, M. Sigel, and J. Mlynek, *Phys. Rep.* **240**, 143 (1994), and references therein.

<sup>4</sup>K. K. Berggren, A. Bard, J. L. Wilbur, J. D. Gillaspay, A. G. Helg, J. J. McClelland, S. L. Rolston, W. D. Phillips, M. Prentiss, and G. M. Whitesides, *Science* **269**, 1255 (1995).

<sup>5</sup>S. Nowak, T. Pfau, and J. Mlynek, *Appl. Phys. B: Lasers Opt.* **63**, 203 (1996); S. Nowak, T. Pfau, and J. Mlynek, *Microelectron. Eng.* **35**, 427 (1997).

<sup>6</sup>K. K. Berggren, R. Younkin, E. Cheung, M. Prentiss, A. J. Black, G. M. Whitesides, D. C. Ralph, C. T. Black, and M. Tinkham, *Adv. Mater.* **9**, 52 (1997); M. Kreis, F. Lison, D. Haubrich, D. Meschede, S. Nowak, T. Pfau, and J. Mlynek, *Appl. Phys. B: Lasers Opt.* **63**, 649 (1996).

<sup>7</sup>R. Younkin, K. K. Berggren, K. S. Johnson, D. C. Ralph, M. Prentiss, and G. M. Whitesides, *Appl. Phys. Lett.* **71**, 1261 (1997).

<sup>8</sup>The energy stored in the internal state of a metastable noble gas atom is as follows:  $\text{He}^* \approx 20$  eV,  $\text{Ne}^* \approx 17$  eV,  $\text{Ar}^* \approx 12$  eV,  $\text{Kr}^* \approx 10$  eV, and  $\text{Xe}^* \approx 8$  eV. Their natural lifetimes are  $\geq 20$  ms, which is much longer than their flight time through a typical apparatus.

<sup>9</sup>D. M. Oro, P. A. Soletsky, X. Zhang, F. B. Dunning, and G. K. Walters, *Phys. Rev. A* **49**, 4703 (1994); Y. Harada, S. Yamamoto, M. Aoki, S. Masuda, T. Ichinokawa, M. Kato, and Y. Sakai, *Nature (London)* **372**, 657 (1994); M. P. Seah and W. A. Dench, *Surf. Interface Anal.* **1**, 2 (1979).

<sup>10</sup>G. Hähner, Ch. Wöll, M. Buck, and M. Grunze, *Langmuir* **9**, 1955 (1993).

<sup>11</sup>K. S. Johnson, K. K. Berggren, A. Black, C. T. Black, A. P. Chu, N. H. Dekker, D. C. Ralph, J. H. Thywissen, R. Younkin, M. Tinkham, M. Prentiss, and G. M. Whitesides, *Appl. Phys. Lett.* **69**, 2773 (1996).

<sup>12</sup>A. P. Chu, K. K. Berggren, K. S. Johnson, and M. Prentiss, *Quantum Semiclass. Opt.* **8**, 521 (1996); A. P. Chu, K. S. Johnson, and M. G. Prentiss, *Opt. Commun.* **134**, 105 (1997).

<sup>13</sup>K. S. Johnson, J. H. Thywissen, N. H. Dekker, K. K. Berggren, A. P. Chu, R. Younkin, and M. Prentiss (unpublished).

<sup>14</sup>Electron beam lithography has demonstrated that both self-assembled monolayers and contamination lithography, the two resist systems that have been used in neutral atom lithography, are capable of supporting  $\sim 6$  nm features. See M. J. Lercel, H. G. Craighead, A. N. Parikh, K. Seshadri, and D. L. Allara, *Appl. Phys. Lett.* **68**, 1504 (1996).

<sup>15</sup>A. N. Broers, W. W. Molzen, J. J. Cuomo, and N. D. Wittels, *Appl. Phys. Lett.* **29**, 596 (1976).

<sup>16</sup>S. J. Rehse, A. D. Glueck, S. A. Lee, A. B. Goulakov, C. S. Menoni, D. C. Ralph, K. S. Johnson, and M. Prentiss, *Appl. Phys. Lett.* **71**, 1427 (1997).

<sup>17</sup>B. Völkel, A. Götzhäuser, H. U. Müller, C. David, and M. Grunze, *J. Vac. Sci. Technol. B* **15**, 2877 (1997).

<sup>18</sup>C. David, D. Kayser, H. U. Müller, B. Völkel, and M. Grunze: "A new method for the manufacture of large area condenser zone plates with small outermost zone widths," in *X-Ray Microscopy and Spectromicroscopy*, edited by J. Thieme, G. Schmal, E. Umbach, and D. Rudolf (Springer, Heidelberg, in press).

<sup>19</sup>B. Jäger, H. Schürmann, H. U. Müller, H.-J. Himmel, M. Neumann, M. Grunze, and Ch. Wöll, *Z. Phys. Chem. (Leipzig)* **202**, 263 (1997).

<sup>20</sup>The diffusion pump oil used in this work was DC705, though similar material is grown with a different oil vapor in other works (see Ref. 16).

- DC705 consists of trimethylpentaphenyltrisiloxane (90%) and poly(phenylmethylsiloxane) (10%).
- <sup>21</sup>S. Schohl, D. Klar, T. Kraft, H. A. J. Meijer, M.-W. Ruf, U. Schmitz, S. J. Smith, and H. Hotop, *Z. Phys. D* **21**, 25 (1991).
- <sup>22</sup>T. A. Savas, S. N. Shah, M. L. Schattensburg, J. M. Carter, and H. I. Smith, *J. Vac. Sci. Technol. B* **13**, 2732 (1995); T. A. Savas, M. L. Schattensburg, J. M. Carter, and H. I. Smith, *ibid.* **14**, 1 (1996).
- <sup>23</sup>The XPS instrument used was a Surface Science Laboratory SSX-100 system.
- <sup>24</sup>The AES instrument used was a Physical Electronics Model 660 Scanning Auger Microprobe; data from this instrument were analyzed with a curve fitting/integration program package, supplied with the system, that uses calculated elemental sensitivity factors.
- <sup>25</sup>These NEXAFS spectra were recorded at the HE-TGM 2 monochromator of the Berlin electron storage ring, BESSY (see Ref. 29). The NEXAFS spectra were recorded at room temperature in the partial electron yield detection mode with a retarding voltage of  $-150$  eV. The NEXAFS data were normalized to the monochromator flux as determined by photon yield from a clean gold surface and background corrected.
- <sup>26</sup>Carbon nanotube tips are fabricated by attaching multiwalled carbon nanotubes to the side of the tip of a conventional silicon cantilever using a soft acrylic adhesive. These nanotubes are strong and flexible, and have a well-defined reproducible geometry, typically with lengths of  $> 1 \mu\text{m}$  and diameters of  $5\text{--}20$  nm. These properties enable them to probe into deep recesses in surface topography. See H. Dai, J. H. Hafner, A. G. Rinzler, D. T. Colbert, and R. E. Smalley, *Nature (London)* **384**, 147 (1996); S. S. Wong, J. D. Harper, P. T. Lansbury, Jr., and C. M. Lieber, *J. Am. Chem. Soc.* **120**, 603 (1998).
- <sup>27</sup>Y. Ochiai, H. Watanabe, J. Fujita, M. Baba, S. Manako, and S. Matsui, *Jpn. J. Appl. Phys., Part 1* **32**, 6147 (1993).
- <sup>28</sup>Exposing samples in the presence of an additional source of oil vapor increases the growth rate of material on the surface. This observation provides further evidence that adsorbed pump fluid is involved in the formation of material on the surface and that the rate of formation is limited, in part, by the availability of material at the surface during exposure.
- <sup>29</sup>J. Stöhr, *NEXAFS Spectroscopy* (Springer, Heidelberg, 1991), p. 284.
- <sup>30</sup>M. J. Lercel, C. S. Whelan, H. G. Craighead, K. Seshadri, and D. L. Allara, *J. Vac. Sci. Technol. B* **14**, 4085 (1996).
- <sup>31</sup>W. M. Moreau, *Semiconductor Lithography: Principles, Practices and Materials* (Plenum, New York, 1988), p. 730.
- <sup>32</sup>G. E. Potter, G. H. Morrison, P. K. Charvat, and A. L. Ruoff, *J. Vac. Sci. Technol. B* **10**, 2398 (1992).
- <sup>33</sup>See, for instance, I. W. Rangelow and H. Löschner, *J. Vac. Sci. Technol. B* **13**, 2394 (1995).